# High-Stress Ice Fracture and Friction

**M. A. Rist**

*Rock and Ice Physics Laboratory, Department of Geological Sciences, University College London, Gower Street, London WC1E 6BT, U.K.*

*Received: October 11, 1996; In Final Form: May 9, 1997*

The fracture and friction of ice have been examined under triaxial compression at rates and temperatures for which the deformation behavior is predominantly brittle−elastic. Strength is limited by rapid, unstable fracture which occurs along cleavage planes that experience the highest resolved shear stress in the case of single crystals and in the direction of maximum bulk shear stress for polycrystals. Fracture propagation is possibly associated with the onset of plastic slip or yielding in both cases. Polycrystalline ice frictional sliding at high rates and/or low temperatures appears to be the result of elastically deforming asperities that undergo shear failure. A well-defined frictional law is apparent in which (shear stress) $\propto$ (normal stress)$^{2/3}$, independent of temperature, surface roughness, and sliding rate, provided deformation remains elastic.

## 1. Introduction

Tensile brittle fracture of single crystals and polycrystalline materials is generally well understood. Failure tends to occur by the unstable (i.e. very rapid) growth of a single flaw that propagates perpendicular to the direction of maximum tension, although in single crystals there is a preference for the cleavage direction. Compressive brittle fracture is less well understood. Under triaxial compression unstable tensile propagation is suppressed, while unstable shear growth of a flaw is not known to occur in an isotropic material. Instead macroscopic fracture requires the interaction and linking of tensile microfractures to form a weakened shear zone along which the failure occurs. This process obviously requires much higher stresses than simple unstable tensile crack propagation. As a single crystal is a macroscopically anisotropic material, a plane of weakness may already exist to facilitate fracture propagation.

Compressive fracture is important because it represents the upper strength limit of a material at high rates of loading. In this paper ice single crystal and polycrystal fracture behavior under triaxial compression is summarized and the influence of this behavior on the high-stress frictional properties of ice is examined. It is observed that ice brittle fracture and frictional sliding are closely related and can be directly compared to the mechanical behavior of hexagonal close-packed metals.

## 2. General Methodology

The mechanical behavior of ice was examined by means of triaxial testing in which a hydrostatic pressure and a uniaxial compressive loading stress were superimposed.[1−5] Deformation rates equivalent to strain rates in the range $10^{-5}$−$10^{-2}$ $s^{-1}$ were applied at temperatures of −20 and −40 °C with confining pressures up to 50 MPa. The aim was to impose conditions that would promote macroscopic material-dependent fracture. The moderate confining pressures were used to suppress the axial tensile splitting that can often arise under uniaxial conditions and to promote a more uniform stress field within the specimen. The results presented here were obtained using two different testing rigs. The first was a gas rig used for studying the deformation of cylindrical polycrystalline specimens, 40 × 100 mm in length, at the lower temperature.[1−4] The second triaxial cell utilized clear silicone oil as a confining medium and incorporated a unique viewing port for direct observation during testing.[5] This latter apparatus, which was limited to confining pressures up to 20 MPa, was the source of the new data presented here on ice single crystal fracture and polycrystal fracture and friction at −20 °C. Rectangular prism specimens 60 × 60 × 120 mm were used in this case to facilitate syn-deformational observation of microcrack and fracture formation through the viewing port using video equipment. The single ice crystals were made by slow, unidirectional freezing of a tank of cold water on which a 10 mm thick single-crystal template had been floated.[6] Polycrystalline ice was made by adding deaerated water to molds containing sieved ice grains.[4]

## 3. Single-Crystal Fracture

Deformation was studied at −20 °C using three different crystal orientations: (i) crystallographic *c*-axis at 45° to the loading direction, (ii) *c*-axis perpendicular to the loading direction, (iii) *c*-axis parallel the loading direction. The 45° orientation was used to promote basal glide in the (0001) plane. The other two orientations, which are unfavorable for this easy glide, were intended to promote fracture or slip along other crystallographic planes, if possible. The following deformation behavior was observed.

**(i) *c*-Axis 45° to Loading Direction.** Fracture occurred along the basal plane at the highest strain rate used, $10^{-2}$ $s^{-1}$, with a confining pressure, $P = 10$ MPa (Figure 1a). The stress−strain behavior, shown in Figure 2, indicates that failure was preceded by almost entirely elastic deformation for one specimen but occurred just after the upper yield point, or peak stress, in another case (tests 9 and 3, respectively). In both instances small cracks, a few millimeters in length, were directly observed to form at differential stresses of 10−14 MPa at low strains, $\epsilon = 0.3$−$0.4\%$, presumably due to nonuniform distortion of the crystal at this high strain rate. Because this implies some nonelastic deformation, the elastic nature of the rising part of the stress−strain curve was verified by placing strain transducers directly on the ice surface which produced a measured elastic modulus of 8.9 GPa, very close to the dynamic elastic modulus for ice.[7] The macroscopic fracture surfaces were typical of those for cleavage fracture in brittle polycrystalline materials such as ice:[8] stepped cleavage surfaces forming a radiating pattern indicative of the nucleation center of the fracture. A large number of small "feather" fractures, over 10 mm long in places and just visible in Figure 1a, formed at right angles to the main

⊗ Abstract published in *Advance ACS Abstracts,* August 1, 1997.

S1089-5647(96)03175-6 CCC: $14.00 

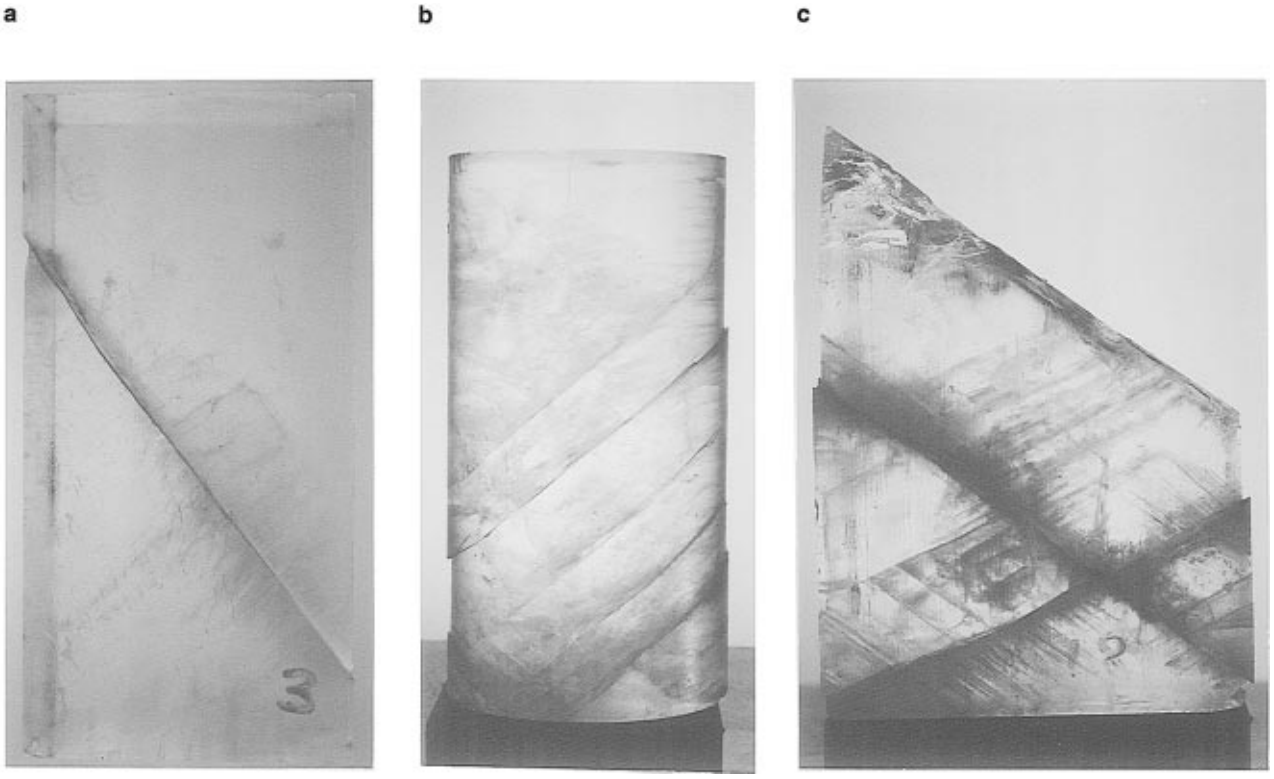


**Figure 1.** Fractured single-crystal ice specimens: (a) fracture along basal plane and associated prismatic "feather" fractures (test 3; *c*-axis at 45° to loading direction); (b and c) fracture along prismatic planes (tests 16 and 18; *c*-axes perpendicular to loading direction).

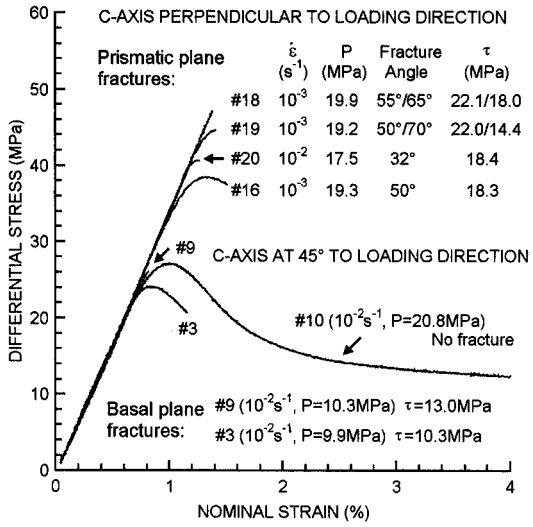


**Figure 2.** Stress−strain curves for single-crystal brittle deformation under triaxial stress at −20 °C. Confining pressure and strain rate are marked for each test. Resolved shear stress, $\tau$, along the fracture plane is also indicated along with the plane orientation, which differed from test to test for the prismatic fractures.

basal plane fracture. On closer inspection these were found to intersect each other at angles of 60° and 120°, indicating that they formed along prismatic $\{10\bar{1}0\}$ planes. It was not possible to distinguish a third cleavage direction on pyramidal planes as observed elsewhere.[8,9] For test 3 small traces of recrystallization, visible under cross-polarized light, were associated with lines of fine gouge and cracking. However, in the case of test 9, almost the entire surface of *one* of the fracture faces displayed extensive recrystallization, not associated with gouge or other visible damage, penetrating some 2−3 mm into the fractured surface in places. Stresses should not have been high enough to induce melting, and this may merely have been annealed gouge.

Macroscopic fracture was suppressed by increasing the confining pressure to 20 MPa (test 10, Figure 2), and the stress−strain curve displayed a characteristic upper yield point.[10] In this case small cracks did not form at low stresses, but rather the first crack was observed to form in the direction of the basal plane just after the peak stress, at $\epsilon = 1.1\%$, presumably triggered by localized yielding. The peak stress reached at the upper yield point is similar to the fracture propagation stress for the brittle specimens. Hence localized yielding not only may create microcracks but could also act to destabilise them and trigger macroscopic fracture.

At lower strain rates, $10^{-3}-10^{-5}$ s$^{-1}$, macroscopic fracture was always suppressed by a confining pressure of 10 MPa, although small cracks still formed, a few millimeters in length, generally in the basal plane or *c*-axis directions. At the lowest strain rate, $10^{-5}$ s$^{-1}$, no visible damage occurred to the specimen when viewed under normal light, but banding *in the direction of the c-axis*, also evident at higher strain rates where the upper yield point was reached, was observed under crossed polarizers. The banding more commonly observed in the basal plane due to slip[11] was not evident here, although it should be noted that the plastic strains imposed during this study were comparatively small (3−4%).

**(ii) *c*-Axis Perpendicular to Loading Direction.** At strain rates of $10^{-2}-10^{-3}$ s$^{-1}$ macroscopic fracture occurred along one or more prismatic planes after predominantly elastic deformation (Figures 1b,c and 2). Fracture was not inhibited by the highest confining pressure that could be imposed by the apparatus, i.e. 20 MPa. The shapes of the stress−strain curves shown in Figure 2 (tests 16, 18, 19, and 20) are such that it seems that an upper yield point is being approached when fracture intercedes. Initial stable cracks were observed to form at small strains of less than 0.5%, as mentioned above.

In all cases the fracture surfaces were along the prismatic planes that experienced the largest shear stresses. For example, in the case of the specimen of test 18 shown in Figure 1c, the

prismatic planes make angles with the loading direction of 65° (resolved shear and normal stresses at failure, $\tau = 18.0$ MPa, $\sigma_n = 58.6$ MPa), 55° ($\tau = 22.1$ MPa, $\sigma_n = 51.5$ MPa), and 5° ($\tau = 4.1$ MPa, $\sigma_n = 20.4$ MPa). Cleavage fractures ought to propagate perpendicular to the direction of minimum compression, i.e. along the prismatic face oriented at 5° to the loading axis. In fact this has not occurred and the 55° face has been exploited, with subsidiary fractures along the 65° face. The association of the fracturing with the maximum shear stress direction suggests that instability may be initiated by a small amount of localized slip in this direction. Other resolved fracture stresses for prismatic fracture are shown in Figure 2, and it is clear that they are all similar, possibly indicating a critical shear stress that is independent of strain rate.

At lower strain rates, $10^{-4}-10^{-5}$ $s^{-1}$, deformation became concentrated, after the peak stress had been attained, into broad bands of intense recrystallization and reorientation. Cavities and vertical fractures, often displaced along the deformation zone, were associated with this banding. None of these features could be systematically associated with any specific crystallographic plane.

**(iii) *c*-Axis Parallel to the Loading Direction.** For loading in this direction much higher loads were attained. Nevertheless, the behavior was always dominated by fracture or slip along a slightly misoriented (or possibly realigned) basal plane. It was not possible to tell if deformation associated with any other crystallographic plane had occurred.

## 4. Polycrystal Fracture

The high-rate fracture behavior of pure isotropic polycrystalline ice under triaxial compression has been reported elsewhere.[1,4,5] At temperatures of −20 and −40 °C, using grain sizes of about 5 and 1 mm, respectively, there is a transition to brittle failure at a strain rate of $10^{-2}$ $s^{-1}$. In both cases failure occurs by sudden shear fracturing at an angle that can be variable at low stresses, but that is generally inclined at about 45° to the direction of maximum compression (the loading axis) at higher stresses. The shear fracture strength (i) appears to become pressure-independent above $P = 5-10$ MPa, (ii) is not accompanied by significant volumetric dilatancy, and (iii) is not suppressed by pressures up to 20 MPa at −20 °C or up to 50 MPa at −40 °C. Durham and others[12] have found similar behavior at much lower temperatures, −115 to −196 °C, at strain rates below $10^{-4}$ $s^{-1}$, conditions under which polycrystal shear fracture is not inhibited by confining pressures up to 350 MPa.

The resolved stresses on the fracture surface for the −20 and −40 °C tests are plotted in Figure 3, assuming fracture angles of 45°. In both cases it appears that a critical shear stress may eventually be reached with $\tau_{max} = 15$ MPa at −20 °C and $\tau_{max} = 30$ MPa at −40 °C. Other tests at lower strain rates in which deformation was macroscopically ductile were also conducted. Extrapolation of this data indicates that the polycrystal yield stresses at −40 and −20 °C for the test strain rate of $10^{-2}$ $s^{-1}$ correspond to the critical shear fracture stresses stated above (see Figure 3). This is borne out by the fact that tests on 1 mm grain-sized ice at −20 °C *did not fracture*, but yielded at the approximate brittle failure stress of the 5 mm grain-sized ice at the same temperature.[5] A larger grain size would have little influence on the yield stress but may promote fracture by allowing larger flaws to nucleate. It appears that propagation of these flaws to form a macroscopic fracture may have been triggered by (localized) yielding.

It is noteworthy that the maximum polycrystal shear stress at −20 °C is close to the critical prismatic shear fracture stress at the same temperature and strain rate (Figures 2 and 3). Whether this is coincidence or whether the single crystal fracture strength has such a direct bearing on polycrystal shear strength is a matter for further investigation.

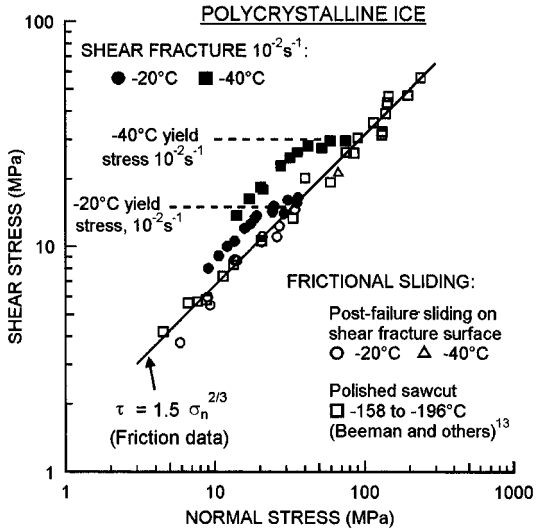


**Figure 3.** Polycrystal friction, fracture, and yield derived from triaxial testing. Friction data points represent resolved stresses for the largest stick−slip event during sliding under various temperatures, pressures, and sliding rates (see text for details). The shear fracture points are peak-resolved fracture stresses at various confining pressures at −20 and −40 °C with a strain rate of $10^{-2}$ $s^{-1}$. The expected upper yield stress in the abscence of factor is also marked on the figure for these temperatures and strain rate.

## 5. Polycrystal Friction

At high stresses, fracture and friction are closely related. At temperatures and sliding rates where frictional heating is insufficient to create a water film, behavior is characterized by stick−slip sliding. Beeman and others[13] have used triaxial apparatus to conduct sliding experiments on polycrystalline ice specimens with inclined polished saw-cut surfaces at low temperatures (−196 to −158 °C) and low sliding rates ($<3 \times 10^{-5}$ $ms^{-1}$). Seemingly erratic pressure-dependent stick−slip behavior was observed. However, by plotting the resolved stresses on the sliding plane at the largest stick−slip event, ignoring tests conducted at pressures high enough to induce a phase change, a very well-defined trend is evident (Figure 3). Frictional stresses can also be deduced from the postfailure stick−slip sliding in our fracture tests at −20 °C, and for a single test at −40 °C. Again by plotting the stresses for the largest stick−slip event if more than one slip event occurred, despite the higher sliding rate ($\approx 10^{-3}$ $ms^{-1}$) and higher temperatures, the trend is practically identical to that of the saw-cut specimen data.

This friction data set therefore covers temperatures from −20 to −196 °C, some 2 orders of stress magnitude, is independent of sliding rate and applies both to rough and to smooth surfaces. The connecting factor covering all this data is the predominantly *elastic-brittle* mechanical behavior of ice at high strain rates and/or low temperatures. As shown in Figure 3 the behavior closely follows the trend $\tau \propto \sigma_n^{2/3}$ (friction coefficient, $\mu \approx 0.4-0.8$). The power exponent is significant because the true contact area, $A$, of a single elastically deforming spherical asperity depends on the applied normal load, $F_n$, as $A \propto F_n^{2/3}$ (Hertzian contact).[14] For multiple contacts the relationship would be the same provided the asperities were of equal height or if increased load did not bring new areas into contact.[15] This situation leads to the same relationship between macroscopic

shear and normal stresses provided the apparent contact area does not alter significantly. However, "real" surfaces usually have a normal or Gaussian distribution of asperity heights so that an increased load does bring new areas into contact. In this case $A \propto F_n$ and $\tau \propto \sigma_n$, Amonton's frictional law. This linear law, which defines a constant value of $\mu$, also applies to plastic and elastoplastic deformation of *any* distribution of asperity heights.[14] For non-Gaussian height distributions of elastic asperities, however, the relationship between $A$ and $F_n$ follows a power law with an exponent whose value lies between 2/3 and unity.[16]

The elastic−brittle behavior of ice single crystals under high-rate compression has been demonstrated in section 3 of this paper. During frictional sliding of a polycrystal, deformation of asperities is likely to be dominated by single crystal deformation. The brittle shearing of these asperities may create an approximately constant asperity height, especially after repeated stick−slip events, explaining the observed power-law dependence of resolved stresses. The friction data plotted in Figure 3 strongly support the suggestion that the brittle fracture of such elastically deforming asperities is the mechanism for the high-stress ice frictional behavior presented here.

The broad temperature independence of ice friction may appear extraordinary, but it is supported by observations made on hexagonal close-packed (hcp) metals, Ti, Zr, Be, Co, in an extensive study by Bowden and Childs.[17] They found no change in frictional behavior from room temperature down to −240 °C. On the other hand, cubic close-packed metals, e.g. Ni, Cu, Au, Ag, and some body-centered cubic metals, e.g. Mo, Fe, displayed a marked transition in $\mu$ at temperatures above about −170 °C. This was due to a change in work hardening rate or a ductile−brittle transition which is not observed in hcp metals or in ice at high rates. Low values of the friction coefficient below $\mu = 1$ are generally only found in the hcp metals, and ice, at these low temperatures. Interestingly, it is the most brittle hcp metals, Co and Be, that give values of $\mu$ (0.55 and 0.75, respectively) that are most similar to those for ice. Polycrystalline Co, like ice, fails by catastrophic shear fracture at 45° to the loading axis in (uniaxial) compression at −196 °C.[17] Basal slip predominates in Co and Be, as for ice, whereas Zr and Ti also have significant slip on prismatic planes,[18] making them less brittle. The low friction coefficients of Be and Co were attributed by Bowden and Childs[17] to failure by shear in the interfacial plane before stresses have built up large enough to cause large-scale yielding or tearing. This is precisely the mechanism proposed here for ice. The elastic−brittle frictional behavior of ice therefore closely resembles that of these hcp metals, the only surprise being that it persists over a much higher and broader homologous temperature range.

## 6. Conclusions

The compressive deformation and friction of ice have been examined at rates and temperatures for which the deformation behavior is predominantly elastic−brittle. Under these conditions the strength of ice is limited by rapid, unstable shear fracture. In the case of single crystals, macroscopic fracture occurs along the basal plane or, if the orientation is unfavorable for basal slip, the prismatic planes. Although apparently tensional in nature, these fractures propagate on the cleavage planes that experience the highest resolved shear stress and are possibly triggered by localized plastic slip. Polycrystal shear fracture also occurs in the direction of bulk maximum shear stress and is possibly associated with the onset of plastic yielding at the highest stresses. At high rates and/or low temperatures, ice frictional sliding appears to be the result of elastically deforming asperities that undergo shear failure. This latter behavior is independent of temperature, surface roughness, and sliding rate, provided the deformation remains elastic, and it resembles friction in hcp metals.

**Acknowledgment.** The support of the UK Natural Environment Research Council and the National Research Council of Canada during the course of much of this work is gratefully acknowledged. Special thanks for much help and personal support go to Prof. S. A. F. Murrell and Dr. P. R Sammonds at University College London and Dr. S. J. Jones, Dr. R. E. Gagnon, and Mr. T. D. Slade at the Institute for Marine Dynamics, Newfoundland.

## References and Notes

(1) Murrell, S. A. F.; Sammonds, P. R.; Rist, M. A. In *Ice Structure Interactions. IUTAM/IAHR Symposium, St John's, Nfd, Canada, 1989*; Jones, S. J., McKenna, R. F., Tillotson, J., Jordaan, I. J., Eds.; Springer-Verlag: Berlin, 1991; p 339.

(2) Sammonds, P. R.; Murrell, S. A. F.; Rist, M. A.; Butler, D. *Cold Reg. Sci. Technol.* **1991**, *19*, 177.

(3) Rist, M. A.; Sammonds, P. R.; Murrell, S. A. F. *Cold Reg. Sci. Technol.* **1991**, *19*, 189.

(4) Rist, M. A.; Murrell, S. A. F. *J. Glaciol.* **1994**, *40*, 305.

(5) Rist, M. A.; Jones, S. J.; Slade, T. D. *Ann. Glaciol.* **1994**, *19*, 131.

(6) Technique developed by R. E. Gagnon, Institute for Marine Dynamics, St John's, Nfd, Canada.

(7) Hobbs, P. V. *Ice Physics*; Clarendon Press: Oxford, 1974.

(8) Wei, Y.; Dempsey, J. P. *J. Mater. Sci.* **1991**, *26*, 5733.

(9) Wakahama, G. *Low Temp. Sci.* **1965**, *A23*, 39.

(10) Jones, S. J.; Glen, J. W. *J. Glaciol.* **1969**, *8*, 463.

(11) Nakaya, U. US Army Snow Ice and Permafrost Research Establishment Report No. 28; US Army Snow Ice and Permafrost Research Establishment: Illinois, 1958.

(12) Durham, W. B.; Heard, H. C.; Kirby, S. H. *J. Geophys. Res*. **1983**, *88*, B377.

(13) Beeman, M.; Durham, W. B.; Kirby, S. H. *J. Geophys. Res.* **1988**, *93*, 7625.

(14) Moore, D. F. *Principles and Applications of Tribology*; Pergamon Press: Oxford, 1975.

(15) Archard, J. F. *J. Appl. Phys.* **1961**, *32*, 1420.

(16) Archard, J. F. *Proc. R. Soc. London* **1957**, *A243*, 190.

(17) Bowden, F. P.; Childs, T. H. C. *Proc. R. Soc. London* **1969**, *A312*, 451.

(18) Partridge, P. G. *Metals Mater.* **1967**, *1*, 169.